Low-Energy Electron Diffraction Amplitudes for a "Bare-Substrate" Model

E. G. McRae

Bell Laboratories, Murray Hill, New Jersey

(Z. Naturforsch. **27 a**, 373—382 [1972]; received 16 November 1971)

Dedicated to Prof. Dr. K. Molière *on his 60-th birthday*

A theory of low-energy electron diffraction (LEED) amplitudes is developed for a model in which the crystal surface is represented by a step-function termination of the bulk crystal potential ("bare-substrate" model). The crystal is considered to be centro-symmetric and it is assumed that either the crystal has a two-fold axis of rotation normal to the surface or the primay beam is normally incident on the surface. The origin of coordinates is taken to lie at a center of symmetry of the substrate crystal. The diffraction amplitude is considered as a function of complex electron energy. For a real potential it is shown to have the following properties:

1. The imaginary part of the amplitude vanishes at each branch point of the amplitude function;
2. There are certain segments of the real-energy axis, called "inactive" segments, throughout which the imaginary part of the amplitude vanishes approximately.

The theoretical results are illustrated by a numerical example. It is suggested that the diffraction amplitude can be represented by a simple expression that has the correct functional form and that satisfies the appropriate dispersion relation. One such expression is proposed and discussed in comparison with exact computational results.

1. Introduction

In a recent paper, Gersten and McRae (GM)[1] treated some general properties of low-energy electron diffraction (LEED) amplitudes. The results of GM refer to a two-dimensionally periodic model crystal consisting of a three-dimensionally periodic substrate and a selvedge (surface region) that is two-dimensionally periodic but of otherwise arbitrary structure. In the present paper we give additional results for a "bare" substrate — i.e. a model in which the substrate-vacuum interface is represented by a potential step in a plane parallel to the surface. The bare-substrate model considered here approximately represents the case of an atomically-clean and unreconstructed crystal surface[2]. The ultimate objective of this kind of study is to develop methods of determining diffraction amplitudes that make maximum use of experimental data and that do not depend heavily on the details of any particular model or method of treatment. We expect that such methods will play an important part in the determination of crystal surface structure by LEED.

The paper by GM[1] deals with the form of the diffraction amplitude, considered as a function of the electron energy. As pointed out by GM, for a real potential the singularities of the amplitude function comprise a sequence of branch points on the real-energy axis and poles corresponding to surface states. The branch points are the thresholds of diffracted beams (vacuum threshold branch points) and the extremities of the band gaps taken along the appropriate one-dimensional section through the substrate band structure (crystal branch points). On the basis of these considerations, GM derived the energy dispersion relation satisfied by diffraction amplitudes for a real potential. Aside from pole terms due to surface states, the dispersion relation is an integral expression for the diffraction amplitudes (or for specific combinations of amplitudes) in terms of their imaginary parts only. One aspect of the dispersion relation that is of particular importance for LEED is that it provides the link between amplitudes for real potentials and those for optical potentials in which the effect of inelastic scattering is represented by a spatially-constant imaginary term ("uniform-absorption" model).

With a view to using the dispersion relation to analyse LEED data, it is of interest to examine the particular properties of the imaginary part of the amplitude considered as a function of electron energy. The motivation for this kind of study may be explained with reference to the two-beam case. This is equivalent to a one-dimensional diffraction problem. In the two-beam case, one can write

Reprint requests to Dr. E. G. McRae, Bell Laboratories 600 Mountain Avenue, *Murray Hill, New Jersey* 07974, *U.S.A.*

down an exact expression for the diffraction amplitude in terms of the amplitude reflection and transmission coefficients of a single atom layer of the crystal[3]. The model, the arrangement of branch points and the form of the amplitude and intensity for a real model potential are sketched in Fig. 1. The indicated form of the amplitude applies for a "natural" choice of origin of coordinates in the plane one-half of one layer spacing above the topmost atom layer, as indicated in Figure 1(a). The important property of the amplitude is that the imaginary part vanishes at each branch point and is zero throughout each segment of the real-energy axis corresponding to "allowed" regions of the band structure. Now if we were given only these properties of the amplitude together with the intensity, we could form a complete and moderately accurate picture of the amplitude by representing the imaginary part with a sequence of loops enclosing the appropriate areas, and then using the dispersion relation to generate the real part. The same procedure could be used for uniform-absorption models provided that the absorptive term of the potential were known.

It is evident from the example that in the two-beam case one can determine the amplitude from knowledge of the intensity, and without calculations involving the scattering potential of the crystal. This is possible because of special properties of two-beam amplitudes that are independent of the details of the potential, namely that the imaginary part vanishes at each branch point and is zero throughout alternate segments between neighboring branch points. It is natural to ask whether similar properties apply also in the many-beam case. In this paper we show that similar properties do in fact apply in the many-beam case provided certain elements of symmetry are present, and we demonstrate by a computational example how these properties might be used to find a useful representation of the diffraction amplitude.

Our results apply to a bare-substrate model having the following elements of symmetry: the substrate must be centro-symmetric and it is required that either there be a two-fold symmetry axis normal to the surface or that the primary beam be normally-incident on the surface. The main result is that for a "natural" choice of origin located at a center of symmetry of the substrate, the imaginary part of the amplitude vanishes at each branch point. This is a direct extension of the two-beam result. We also show that under certain conditions the imaginary part of the amplitude can be expected to have very small values along an entire segment of the real-energy axis between two neighboring branch points. In applications of the dispersion relation, the integral along a segment in which this condition applies makes only a very small contribution to the amplitude; we refer to such segments as "inactive" segments. The existence of inactive segments is the many-beam extension of the two-beam result that the imaginary part of the amplitude vanishes in alternate segments. The above results are derived in Sec. 2. In Sec. 3, the results are illustrated by a numerical example. Section 4 deals with the representation of diffraction amplitudes dy a simple expression.

2. Theory

2.1. Notation

The notations used here are as defined by GM[1], but some simplifications are possible because of the extra symmetry specified in Section 1.

The positive Z-direction is the direction of the inward surface normal.

$E = E' + iE''$: electron energy (here and elsewhere in this paper, (′) and (″) denote real and imaginary parts, respectively).

$\boldsymbol{K}^{\pm} \equiv (\boldsymbol{K}_{\|} + 2\pi\boldsymbol{G}_{\|}, \pm K_z)$: propagation vectors of ingoing (+) and outgoing (−) plane waves in vacuum. The projections on the surface and on the inward surface normal are indicated. $\boldsymbol{G}_{\|}$ is a vector of the reciprocal net of the surface. There is one pair of plane waves for each value of $\boldsymbol{G}_{\|}$. $\boldsymbol{K}_{\|}$ is the surface projection of the propagation vectors for the pair of plane waves corresponding to $\boldsymbol{G}_{\|} = 0$. Throughout this paper $\boldsymbol{K}_{\|}$ stands for a fixed pair of parameters. In GM, there are given some relations between quantities corresponding to $+\boldsymbol{K}_{\|}$ and $-\boldsymbol{K}_{\|}$, respectively, but in the present paper the dependence on the sign of $\boldsymbol{K}_{\|}$ is trivial because of the symmetry specified in Sec. 1; therefore, it is nowhere necessary to indicate functional dependence on $\boldsymbol{K}_{\|}$.

$\boldsymbol{k}^{\pm} = (\boldsymbol{K}_{\|} + 2\pi\boldsymbol{G}_{\|}, k_z^{\pm})$: propagation vectors of physical (+) and unphysical (−) Bloch waves in the substrate.

$\psi^{\pm}(E, \boldsymbol{R}) \equiv K_z^{-1/2} \exp(i\boldsymbol{K}^{\pm} \cdot \boldsymbol{R})$: plane waves in vacuum. For symmetrical situations — e.g. normal incidence — the totally-symmetric combination of plane waves is understood.

$\varphi^{\pm}(E, \boldsymbol{R})$: physical (+) and unphysical (−) totally-symmetric Bloch waves.

$\mathbf{a}^{\pm}, \mathbf{a} \equiv \begin{bmatrix} \mathbf{a}^{+} \\ \mathbf{a}^{-} \end{bmatrix}$: coefficient vectors for ingoing (+) and outgoing (−) plane waves. It is specified that corresponding elements of $\mathbf{a}^{+}$ and $\mathbf{a}^{-}$ are coefficients of the plane waves with propagation-vector components $+K_z$ and $-K_z$, respectively.

$\mathbf{b}^{\pm}, \mathbf{b} \equiv \begin{bmatrix} \mathbf{b}^{+} \\ \mathbf{b}^{-} \end{bmatrix}$: coefficient vectors for Bloch waves. It is specified that corresponding elements of $\mathbf{b}^{+}$ and $\mathbf{b}^{-}$ are coefficients of the Bloch waves with propagation-vector components k_z^{+} and k_z^{-}, respectively.

$\mathbf{a} = \mathbf{M}\,\mathbf{b}, \mathbf{M} = \begin{bmatrix} \mathbf{M}^{\mathrm{I}} & \mathbf{M}^{\mathrm{II}} \\ \mathbf{M}^{\mathrm{III}} & \mathbf{M}^{\mathrm{IV}} \end{bmatrix}$: matching matrix.

$\mathbf{a}^{-} = \mathbf{T}\mathbf{a}^{+}, \mathbf{T} = \mathbf{M}^{\mathrm{III}}\,\mathbf{M}^{\mathrm{I}-1}$: diffraction amplitude matrix. The subscript (+) is added where necessary to indicate the physical boundary conditions apply.

In all of the above notations, dependence on the electron energy E is implied and is indicated explicitly where necessary.

2.2. Behavior Near Branch Points

We consider, diffraction by a real potential corresponding to a bare-substrate model under the conditions specified in Sec. 1: centro-symmetric substrate, either a two-fold axis normal to the surface or normal incidence. These conditions mean that the Bloch wave-vector components $k_z^{\pm}$ are related to each other according to an expression of the form $k_z^{\pm} = \pm k_z$. Correspondingly, the totally-symmetric physical and unphysical Bloch waves $\varphi^{\pm}$ are related to each other according to

$$\varphi^{+}(E, \boldsymbol{R}) = \varphi^{-}(E, -\boldsymbol{R}), \tag{1}$$

provided that the origin of coordinates is chosen to be a center of symmetry of the substrate crystal. This is the "natural" choice of origin, and is adopted throughout this paper. A further consequence of the stated symmetry conditions is that the symmetries of the matching and amplitude matrices on the complex-energy plane, as given by .GM[1], reduce in the present instance to $\mathbf{M}(E^{*}) = \mathbf{M}(E)^{*}$ and $\mathbf{T}_{+}(E^{*}) = \mathbf{T}_{+}(E)^{*}$, where (*) denotes the complex conjugate.

We wish to examine the imaginary part of the physical diffraction amplitude function $T_{+}(E)$. To do this we need the following property of the matching matrix:

$$\mathbf{M} = \mathbf{C}\,\mathbf{M}\,\mathbf{C}, \tag{2}$$

$$\mathbf{C} = \begin{bmatrix} \mathbf{0} & \mathbf{I} \\ \mathbf{I} & \mathbf{0} \end{bmatrix}, \tag{3}$$

where $\mathbf{0}$ and $\mathbf{I}$ are respectively null and unit matrices.

Eq. (2) applies under the stated symmetry conditions, provided that the matching plane terminating the crystal is taken to pass through a center of symmetry of the substrate without cutting through any atoms. Eq. (2) follows from Eq. (1); if we consider the plane-wave decomposition of the corresponding physical and unphysical Bloch waves $\varphi^{\pm}$ on the matching plane, we see that the Bloch wave φ^{-} has the same decomposition as does φ^{+} with the corresponding plane waves ψ^{+} and ψ^{-} interchanged.

Let us now consider particularly the behavior of the amplitude near the branch points. First we show that *the imaginary part of the amplitude vanishes at each branch point.* At a crystal branch point, for instance, there is a physical Bloch wave φ^{+} that is identical to the corresponding unphysical one φ^{-}. At the branch point the wave field outside the crystal is not affected by interchanging the corresponding physical and unphysical Bloch waves, so there are two columns of the matching matrix that are proportional to each other. Thus at the crystal branch point E_{B} we have

$$\det \mathbf{M}(E_{\mathrm{B}}) = 0. \tag{4}$$

Now let us write the matching equation in the form

$$\mathbf{b} = \mathbf{M}^{-1}\,\mathbf{a} \tag{5}$$

or equivalently

$$(\det \mathbf{M})\,\mathbf{b} = \overline{\mathbf{M}}\,\mathbf{a}, \tag{6}$$

where $\overline{\mathbf{M}}$ is the matrix formed from $\mathbf{M}$ by replacing each element by its cofactor and transposing. In order that the Bloch coefficient vector $\mathbf{b}$ be finite at the branch point, we have in view of Eq. (4):

$$\overline{\mathbf{M}}(E_{\mathrm{B}})\,\mathbf{a}(E_{\mathrm{B}}) = \mathbf{0}. \tag{7}$$

The form of $\overline{\mathbf{M}}(E)$ may be found with the aid of an identity given WATTS[4]. The result is

$$\overline{\mathbf{M}} = \begin{bmatrix} \mathbf{A} & -\mathbf{M}^{\mathrm{I}-1}\,\mathbf{M}^{\mathrm{II}}\,\mathbf{A} \\ -\mathbf{A}\,\mathbf{M}^{\mathrm{II}}\,\mathbf{M}^{\mathrm{I}-1} & \mathbf{A} \end{bmatrix} \tag{8}$$

with

$$\mathbf{A} = (\det \mathbf{M})(\mathbf{M}^{\mathrm{I}} - \mathbf{M}^{\mathrm{II}}\,\mathbf{M}^{\mathrm{I}-1}\,\mathbf{M}^{\mathrm{II}})^{-1}\,.$$

If we put Eq. (8) into Eq. (7) and then use the definition of the diffraction amplitude matrix $\mathbf{T}(E)$, we get

$$\mathbf{T}(E_{\mathrm{B}}) = \mathbf{T}(E_{\mathrm{B}})^{-1}\,. \tag{9}$$

This is a relation that can be satisfied only by a real matrix. Actually, time-reversal symmetry combined with the extra elements of symmetry specified in this paper implies that $\mathbf{T}(E)$ is symmetric, so $\mathbf{T}(E_{\mathrm{B}})$ is orthogonal.

The same argument goes through in the case of a vacuum threshold branch point E_{B} except that in this case the relation analogous to Eq. (4) is

$$\det \mathbf{M}(E_{\mathrm{B}})^{-1} = 0\,. \tag{10}$$

The result is again that $\mathbf{T}(E_{\mathrm{B}})$ is real.

We now consider the behavior of the amplitude around the branch points. This is given generally by

$$T(E) = T(E_{\mathrm{B}}) + \tau(E - E_{\mathrm{B}})^{1/2}\,. \tag{11}$$

As $T(E_{\mathrm{B}})$ is real as shown above and E_{B} is real, it follows that the expansion coefficient τ must be either real or imaginary.

To find out whether τ is real or imaginary in any particular case, we consider the expansion of either of the functions $K_z(E)$ or $k_z(E)$ about one of its branch points. For example, for energies E in the vicinity of the branch point E_{B} of $k_z(E)$ (a crystal branch point) we can write

$$(E - E_{\mathrm{B}})^{1/2} = \left(\frac{1}{2}\,\frac{\mathrm{d}^2E}{\mathrm{d}k_z^2}\bigg|_{\mathrm{B}}\right)^{1/2}[k_z(E) - k_z(E_{\mathrm{B}})]\,. \tag{12}$$

We consider energies on any sheet (including the physical sheet) on which the imaginary part of the expression in brackets is positive. If the second derivative of the energy at the branch point in Eq. (12) is positive, then the imaginary part of $(E - E_{\mathrm{B}})^{1/2}$ is positive since $\mathrm{Im}\,k_z > 0$ applies, so we have $(E^* - E_{\mathrm{B}})^{1/2} = -[(E - E_{\mathrm{B}})^{1/2}]^*$. We refer to branch points near which this relation is satisfied as "positive" branch points meaning that the second derivative of the energy in Eq. (12) is positive; in GM[1] and in this paper, positive branch points are shown diagrammatically with the cut extending to higher energies. On the other hand, if the second derivative in Eq. (12) is negative ("negative" branch points, cut extending to lower energies) the real part of $(E - E_{\mathrm{B}})^{1/2}$ is negative so we have $(E^* - E_{\mathrm{B}})^{1/2} = [(E - E_{\mathrm{B}})^{1/2}]^*$. Similar remarks apply to the function $K_z(E)$, although in this case all of the branch points are positive ones. Let us now consider the amplitudes for energies E and E^* in the vicinity of a branch point as sketched in Fig. 2. The branch point labelled 2 in Fig. 2 is a positive branch point lying on an already-cut portion of the real axis. If we encircle the branch point following the path indicated in Fig. 2, starting on the physical sheet, we will pass on to an unphysical sheet upon crossing the cut. Combining Eq. (11) with the relation $\mathbf{T}_+(E^*) = \mathbf{T}_+(E)^*$, we get $\tau = -\tau^*$ so τ must be real. A similar argument for the branch point labelled 3 in Fig. 2 — a negative branch point on an already-cut portion of the real axis — shows that for this case the expansion coefficient is imaginary. The cases represented by points 2 and 3 in Fig. 2, where the branch points lie on cut portions of the real axis, are the ones most often encountered in practice, and for these we have that for positive (negative) branch points the expansion coefficient τ is real (imaginary). The exceptional case, represented by the branch point labelled 1 in Fig. 2, is that of a branch point on an uncut portion of the real axis. This could be e.g. a vacuum threshold branch point. In this case a discussion like the one given above for branch point 2 leads to the result that for a positive (negative) branch point on an uncut portion of the real axis, the expansion coefficient τ is imaginary (real).

2.3. Inactive Segments

We propose here that there are some segments of the real-energy axis that are inactive in the sense that the imaginary part of the amplitude is very small along the entire segment. This proposal is based on the result that in each segment the imaginary part of the amplitude vanishes in a particular approximation relating to the matching of plane waves and Bloch waves.

To give a precise statement of our result, some preliminary statements and definitions are needed. Referring to the complex-energy plane, we wish to deal with the behavior of the imaginary part of the amplitude along the upper edge of the cut running along the real axis. Thus E and E^* are to be interpreted as limits as $\varepsilon \to +0$ of $E' + i\varepsilon$ and

$E' - i\varepsilon$, respectively. Suppose that the wave field in vacuum is represented as the superposition of $2n$ plane waves (n ingoing and n outgoing) and the wave field in the substrate as the superposition of $2n$ Bloch waves (n physical and n unphysical). We define propagating and nonpropagating (i.e., evanescent) waves as follows. A plane wave is propagating (nonpropagating) if its propagation vector satisfies

$$K_z(E^*) = -K_z(E) \quad [K_z(E^*) = K_z(E)];$$

a similar definition applies to Bloch waves. The number of propagating ingoing plane waves is denoted by n_A ($n_A \leqq n$) and the number of propagating physical Bloch waves by n_B ($n_B \leqq n$). In this paper each propagating ingoing plane wave is represented diagrammatically by a vacuum cut and each propagating physical Bloch wave by a crystal cut. The order of a segment is defined to be the smaller of the numbers n_A and n_B, and is denoted by $n_<$. We can specify a particular kind of truncation of the $2n \times 2n$ matching matrix in terms of $2n \times 2n$ projection matrices defined as follows. Let $\mathbf{A}(n')$ ($n' \leqq n_A$) denote a projection matrix that, multiplied into $\mathbf{a}$, picks out the coefficients of n' ingoing propagating waves and the coefficients of the corresponding n' outgoing propagating waves and replaces the other coefficients by zero. Similarly, let $\mathbf{B}(n')$ ($n' \leqq n_B$) denote a projection matrix that picks out the coefficients of n' physical propagating Bloch waves and of the corresponding n' unphysical propagating Bloch waves from $\mathbf{b}$. We are interested in the kind of truncation of the matching matrix $\mathbf{M}$ that is obtained by replacing it with $\mathbf{A}(n')\,\mathbf{M}\,\mathbf{B}(n')$ and then reducing its order to $2n' \times 2n'$ by deleting all null elements. The approximation involved in using this truncated matrix in place of $\mathbf{M}$ in to calculate the amplitude matrix $\mathbf{T}$ may be termed an n'th-order matching approximation.

We can now state our result in terms of the above definitions: *in an $n_<$th-order segment,* Im $T_+(E)$ *vanishes in any possible $n_<$th-order matching approximation.*

To derive the above result we compare expressions for the wave field at conjugate energies E and E^*, respectively just above and just below the cut. The wave field Ψ in vacuum and the wave field Φ in the substrate have the expansions

$$\Psi(E, \boldsymbol{R}) = \widetilde{\boldsymbol{\Psi}}(E, \boldsymbol{R})\,\mathbf{a}(E), \tag{13}$$

$$\Phi(E, \boldsymbol{R}) = \widetilde{\boldsymbol{\Phi}}(E, \boldsymbol{R})\,\mathbf{b}(E). \tag{14}$$

Here, $\boldsymbol{\Psi}$ is a column vector whose elements are plane waves, $\boldsymbol{\Phi}$ is a column vector whose elements are Bloch waves and ($\sim$) denotes the matrix transpose. Now the effect of replacing E by E^* is to replace each ingoing propagating plane wave with the corresponding outgoing one and each physical propagating Bloch wave with corresponding unphysical one. Thus in view of the definitions of the projection matrices $\mathbf{A}$ and $\mathbf{B}$ and of the matrix $\mathbf{C}$ [Eq. (3)], we can write

$$\Psi(E^*, \boldsymbol{R}) = \widetilde{\boldsymbol{\Psi}}(E, \boldsymbol{R})[\mathbf{C}\,\mathbf{A}(n_A) + \mathbf{I} - \mathbf{A}(n_A)]\,\mathbf{a}(E^*), \tag{15}$$

$$\Phi(E^*, \boldsymbol{R}) = \widetilde{\boldsymbol{\Phi}}(E, \boldsymbol{R})[(\mathbf{C}\,\mathbf{B}(n_B) + \mathbf{I} - \mathbf{B}(n_B)]\,\mathbf{b}(E^*), \tag{16}$$

where $\mathbf{I}$ is here the $2n \times 2n$ unit matrix. The coefficient vectors are related to each other through the matching matrix, so we have

$$\begin{aligned}[\mathbf{C}\,\mathbf{A}(n_A) + \mathbf{I} - \mathbf{A}(n_A)]\,\mathbf{a}(E^*) \\ = [\mathbf{C}\,\mathbf{A}(n_A) + \mathbf{I} - \mathbf{A}(n_A)]\,\mathbf{M}(E^*)\,\mathbf{b}(E^*) \\ = \mathbf{M}(E)\,[\mathbf{C}\,\mathbf{B}(n_B) + \mathbf{I} - \mathbf{B}(n_B)]\,\mathbf{b}(E^*).\end{aligned} \tag{17}$$

The matrices $\mathbf{A}$, $\mathbf{B}$ and $\mathbf{C}$ have special properties that follow from their definitions:

$$\mathbf{A}^2 = \mathbf{A},\ \mathbf{B}^2 = \mathbf{B},\ \mathbf{C}^2 = \mathbf{I},\ \mathbf{A}\,\mathbf{C} = \mathbf{C}\,\mathbf{A},\ \mathbf{B}\,\mathbf{C} = \mathbf{C}\,\mathbf{B}.$$

Using these relations together with Eq. (17) and then recalling Eq. (2), we get

$$\begin{aligned}\mathbf{A}(n_A)\,\mathbf{M}(E^*)\,\mathbf{B}(n_B) &= \mathbf{A}(n_A)\,\mathbf{C}\mathbf{M}(E)\,\mathbf{C}\mathbf{B}(n_B) \\ &= \mathbf{A}(n_A)\,\mathbf{M}(E)\,\mathbf{B}(n_B).\end{aligned} \tag{18}$$

The equalities still apply if n_A and n_B are both replaced by $n_<$. This result combined with the relation $\mathbf{M}(E^*) = \mathbf{M}(E)^*$ shows that the truncated matching matrix is real. Thus the diffraction amplitude matrix is real in the $n_<$th-order matching approximation.

From the above discussion, a given segment of order $n_<$ can be described accurately as being inactive to the extent that the $n_<$th-order matching approximation holds good. The question is — under what conditions does this matching approximation apply? One obvious circumstance in which it does apply is that in which the $2n$-beam case applies and $n_< = n$. In the two-beam case, for example, the segments are alternately of order 0 (band gaps)

and 1 ("allowed" regions) and the imaginary part of the amplitude vanishes identically in each segment of order 1 (Fig. 1). Now a $2n$-beam approximation should be a good one if it takes into account all plane waves and all Bloch waves whose thresholds lie to the low-energy side of the particular energy range under consideration. Thus

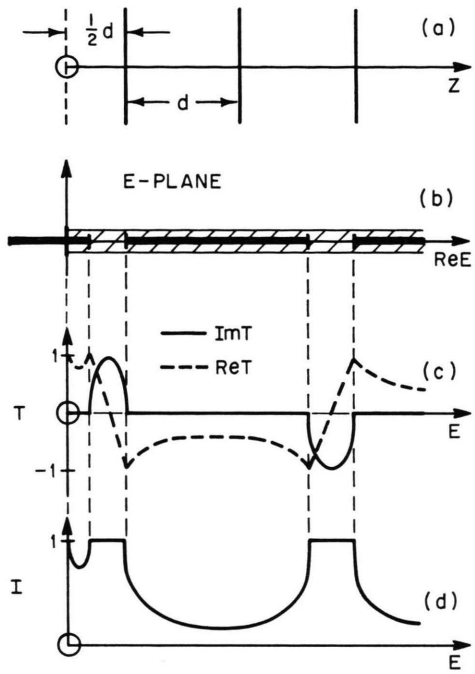

Fig. 1. Sketch of the two-beam model and results. (a) Model. Thick lines denote atom layers parallel to the crystal surface. The positive Z-direction is the inward surface normal. The origin of coordinates 0 lies on the $z = 0$ plane indicated by the broken line. (b) Arrangement of branch points and cuts on the complex-energy plane. Branch points are indicated by solid vertical bars. The vacuum cut extends from the vacuum level to higher energies and is indicated by a shaded horizontal bar. The crystal cut extends over "allowed" regions of the band-structure section and is indicated by the solid horizontal bar. (c) Form of the amplitude function $T(E)$ (E = electron energy). (d) Form of the intensity $I(E)$.

we propose the following rule, to be checked by computation: let N_A denote the number of vacuum threshold branch points and N_B the number of crystal threshold branch points on the low-energy side of the center of a particular segment of order $n_<$; then the imaginary part of the amplitude is approximately zero throughout this segment, provided

$$N_A = N_B = n_< . \tag{19}$$

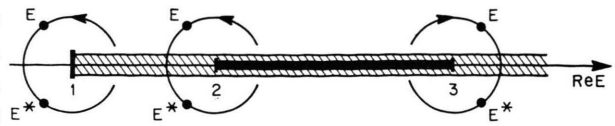

Fig. 2. Illustration of a discussion of the amplitude in the vicinity of branch points. The branch points are indicated by solid vertical bars and the cuts are indicated by horizontal shaded and solid bars.

3. Numerical Example

Our results may be summarized and illustrated by a numerical example. Figure 3 shows the result of a normal incidence computation of the

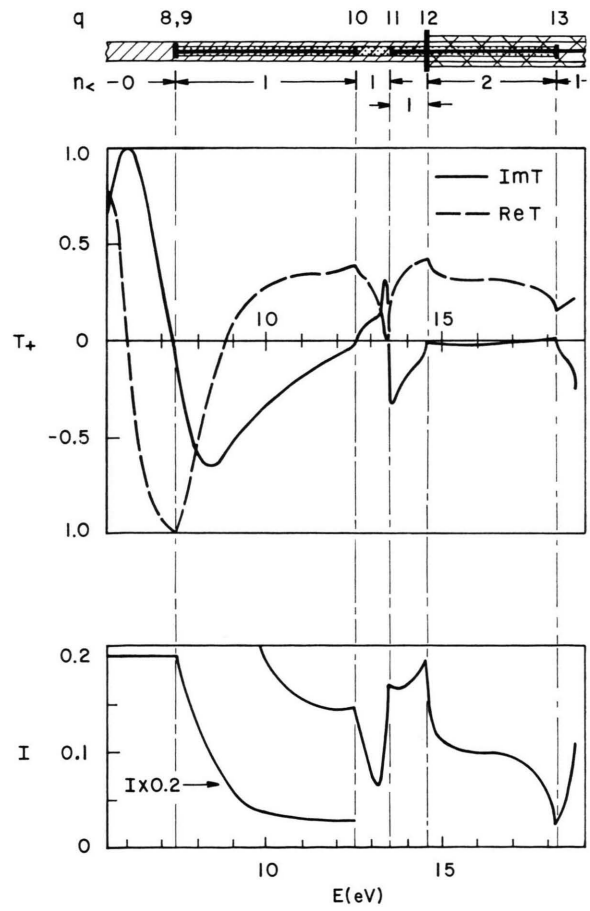

Fig. 3. The amplitude (top f ame) and intensity (bottom frame) calculated as a function of electron energy for a model representing tungsten (001) surface (see the text for a full description of the computation). The diagram at the top of the figure shows the arrangement of branch points. The vacuum branch cuts are indicated by shaded horizontal bars, the crystal branch cuts by stippled and solid horizontal bars. The serial numbers q of the branch points and segments, and the orders $n_<$ of the segments, are indicated.

00 amplitude function $T_+(E)$ and the corresponding intensity $I(E)$ for a "muffin tin" model representing tungsten (001) surface. The model and method of computation are as described previously by JENNINGS and MCRAE[5]. In the present case the step-potential termination of the crystal was assigned a height of 19.7 eV. This is considerably larger than the value 16.0 eV that was adopted previously[5] to fit the observed work function for tungsten (001). The higher value adopted here does not give such good agreement with the observed peak locations in the intensity curve, but as will be made clear below it is a suitable choice for purposes of illustration. The matching plane was a symmetry plane parallel to the (001) surface, and the origin of coordinates was taken to be a center of symmetry of the substrate. To bring out interesting details, the present computation was made at relatively small energy intervals (0.02 ryd, approximately 0.3 eV). Figure 3 includes a diagram of the arrangement of branch points in the energy range of the computation. The corresponding details of the band structure may be found in the paper cited[5]. The serial number of the branch points and segments of the real axis are indicated at the top of Figure 3. The qth segment is taken to extend to the high-energy side of the qth branch point. The segments are marked off and labeled with their respective orders $n_<$ ($n_<$ is the number of propagating plane waves or Bloch waves, whichever is the lesser).

The chief result from Sec. 2.2 is that under certain conditions satisfied in the case of the present computation, the imaginary part of the amplitude vanishes at each branch point. This result is definitely confirmed and illustrated by the computed amplitude shown in Figure 3. Further deductions about the amplitude (Sec. 2.2) are illustrated by the finer details of the computation. In the vicinity of each of the branch points in the range of computation ($q = 8-13$) the amplitude appears within the uncertainty stemming from the computational interval to have the form indicated by Eq. (11) with the coefficient τ real or imaginary according to our criterion of positive and negative branch points. This is shown especially clearly in the case of branch points 12 and 13, which are respectively positive and negative ones.

In Sec. 2.3 it is proposed that there are "inactive" segments along which the imaginary part of the amplitude is very small, and a criterion for such segments [Eq. (19)] is given. Figure 3 contains one segment (segment 12) to which the designation "inactive" definitely applies. Thus the computation confirms the existence of inactive segments. However, the usefulness of the criterion, Eq. (19), is not definitely confirmed. In the case represented in Fig. 3, examination of the band structure[5] shows that there are three crystal threshold branch points and two vacuum threshold branch points below 20 eV. The three crystal thresholds lie below the energy range represented in Figure 3. There is one vacuum threshold at the vacuum level and one vacuum threshold (branch point 12) in the energy range of Figure 3. Thus Eq. (19) is not satisfied for any segment shown in Fig. 3, although the segment identified as inactive is the one in which Eq. (19) is most nearly satisfied (segment 12, $N_A = 2$, $N_B = 3$, $n_< = 2$). The discrepancy might be due to a peculiarity of the band structure. The Bloch wave with a low-energy threshold that would be most plausibly omitted in a second-order matching approximation is an evanescent Bloch wave corresponding to a band gap of enermous width extending upwards from the "flat" d-band. The entire energy range of computation in Fig. 3 lies inside this band gap. One may speculate that omission of such wide-gap evanescent Bloch waves might not have a very important effect in the matching approximation, in which case it would be more appropriate to assign to N_B the value 2 rather than 3.

4. Representation of Diffraction Amplitudes

We wish to study the possibility of parameterizing the diffraction amplitude with a simple expression of the correct functional form. The salient property of the diffraction amplitude for the bare-substrate model treated here is that the imaginary part of the amplitude vanishes at each branch point. It should be possible to fit the diffraction amplitude function with any one of a variety of expressions that have this property and at the same time satisfy the dispersion relation[1]. We here examine one possible expression in which the imaginary part of the amplitude in each segment is represented by a loop like a semicircle.

We suppose that along the qth segment $\mathrm{Im}\, T_+(E')$ is represented by $[1 - s_q(E')^2]^{1/2} \times$ constant where

$s_q(E)$ is analytic within the segment and is of modulus unity at its extremities. Upon expanding $s_q(E)$ about the center E_q^0 of the segment and keeping the first two terms, we get in view of the stated requirements:

$$s_q(E) = 2(E - E_q^0)/(E_{q+1} - E_q). \tag{20}$$

The branch-cut integral can be reduced to the tabulated integral[6]

$$\frac{1}{\pi}\int_{-1}^{+1} \frac{(1-x^2)^{1/2}\,\mathrm{d}x}{x - z} = \pm z + (z^2 - 1)^{1/2} \tag{21}$$

so the dispersion relation gives (omitting pole terms)

$$T_+(E) = \sum_q \frac{4Q_q}{E_{q+1} - E_q}\{\pm s_q(E) + [s_q(E)^2 - 1]^{1/2}\} \tag{22}$$

where Q_q is a segment "strength" given by

$$Q_q = \frac{1}{\pi}\int_{E_q}^{E_{q+1}} \mathrm{Im}\; T_+(E')\,\mathrm{d}E'. \tag{23}$$

For a uniform-absorption model represented by the potential

$$U(E', \boldsymbol{R}) = U'(E', \boldsymbol{R}) + i\,U''(E') \tag{24}$$

where the segment parameters are determined by the real part U', the amplitude for energy E' is obtained from Eq. (22) by inserting

$$E = E' + i\,U''(E').$$

As the absorptive term U'' becomes large, the expression for the amplitude become less sensitive to details of the form of variation of $\mathrm{Im}\,T_+(E')$ within each segment. Thus Eq. (22) may be viewed as a strong-absorption formula. In the limit in which $U''(E')$ is much larger than any segment in the vicinity of E', Eq. (22) reduces to a strong-absorption formula essentially equivalent to the result obtained by SLATER[7] for the two-beam case[1]:

$$T_+(E) = \sum_q \frac{Q_q}{E_q^0 - E}. \tag{25}$$

The Slater-type strong-absorption formula, Eq. (25) may be obtained directly from the dispersion relation by representing $\mathrm{Im}\,T_+(E')$ with a set of delta functions located at the segment centers. The formula proposed here, Eq. (22), contains the same number of parameters as does Eq. (25), but an improvement may be claimed on the ground that a loop like a semicircle is a more realistic representation of the form of $\mathrm{Im}\,T_+(E')$ within a segment than is a delta function. In fact we expect Eq. (22) to be a moderately accurate representation even for a real potential (no absorption).

To examine the possibility of representing amplitudes for a real potential by Eq. (22), we have applied it in an attempt to duplicate the computed amplitude shown in Figure 3. The branch-point locations and strength factors Q_q given by the exact computation were used, and the contribution to the amplitude from segments outside the range of computation were represented by a real, constant background term equal to 0.25. The upper sign in Eq. (22) was adopted for every segment except the lowest-energy one in the range of computation; tests showed that any other choice of signs gives results quite unlike the computed ones.

Used in this way, Eq. (22) gives a recognizable facsimile of the computed amplitude throughout most of the energy range of Fig. 3, but it completely fails to reproduce the sharp variation of amplitude near branch point 11. We interpret this sharp feature of the exact computation as a surface-state resonance associated with the vacuum threshold at slightly higher energy (branch point 12). The resonance is apparently "locked on" to the crystal branch point (branch point 11) in the way described by GM[1]. According to this interpretation the expression for the amplitude in the vicinity of the branch point E_B should contain a term of the form

$$[\alpha + \beta(E - E_\mathrm{B})^{1/2} + \gamma(E - E_\mathrm{B})]^{-1} \tag{26}$$

with $\alpha = T_+(E_\mathrm{B}) - T_+^0(E_\mathrm{B})$ [T_+^0 being as given by Eq. (22)], $\beta = -\alpha^2\tau$ and $\gamma = [\alpha + \beta(E_\mathrm{p} - E_\mathrm{B})^{1/2}]/(E_\mathrm{B} - E_\mathrm{p})$ where $E_\mathrm{p} = E_p' + iE_p''$ denotes the location of the resonance pole. The branch point 11 is a positive branch point lying on an already-cut portion of the real axis, so according to our discussion in Sec. 2.2 the expansion coefficient τ is real.

The resonance expression, Eq. (26), is capable of reproducing the amplitude variation given according to exact computation near branch point 11. Parameter values that give roughly the correct location, width and shape of the resonance are:

$$E_p' - E_\mathrm{B} = -0.14\,\mathrm{eV}, \quad E_p'' = -0.23\,\mathrm{eV},$$
$$\alpha\tau = 1.8\,(\mathrm{eV})^{-1/2}.$$

Figure 4 shows the result of calculating the amplitude and intensity by Eq. (22), with an added resonance term of the form of Eq. (26). In this calculation α was assigned the value -0.14 and the magnitudes of the strength factors in Eq. (22) were reduced to preserve the correct values of the Q's defined by Eq. (23) (only segments 10 and 11 are affected by the resonance). The shape of the resonance term alone is shown in an inset in Fig. 4, top frame. The occurrence of a single asymmetrical minimum in the real part of the amplitude (Fig. 4 inset) can only be obtained as a consequence of the interaction between the pole and the branch point, and this feature is present in the computed curve (Fig. 3).

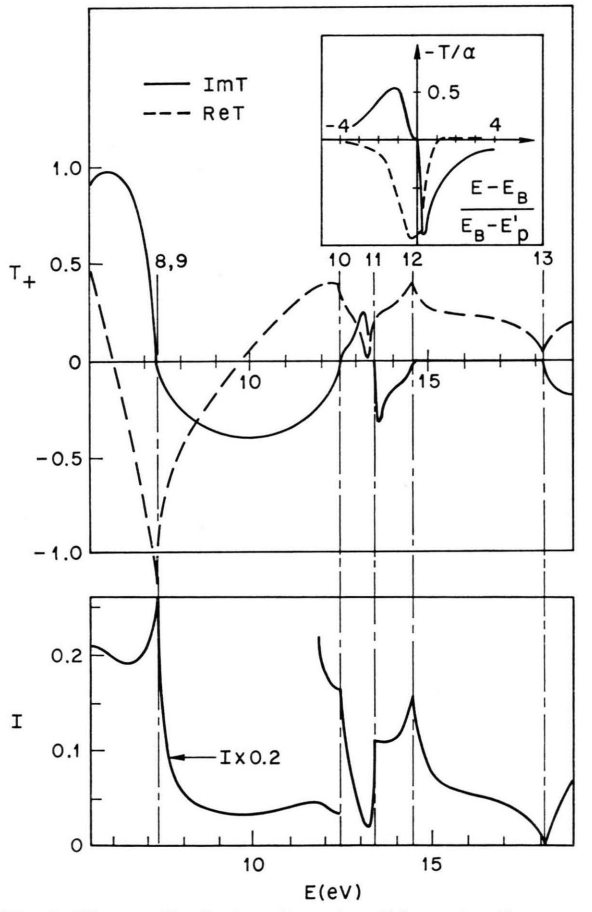

Fig. 4. The amplitude (top frame) and intensity (bottom frame) calculated from Eq. (22) with an added resonance term of the form indicated by Eq. (26) (inset, top frame). The serial numbers of the branch points and segments are indicated and are the same as in Figure 3. The parameters of the calculation were chosen to correspond to the exact computation shown in Figure 3.

The accuracy of a representation based on Eq. (22) (modified by an added resonance term) may be gauged by comparing Fig. 4 with the exact computational results (Fig. 3). The proposed representation has two obvious flaws. In the first place the real part of the amplitude is too small at the high-energy end. This means that the background term due to higher-energy segments is not a constant as assumed, but increases with energy. This is of course what one would expect if the contributions from nearby higher-energy segments were predominantly positive. The other flaw is the unduly spikey shape of the real part of the amplitude and of the intensity curves near branch points 8 and 12. This could perhaps be cured by modifying the shape of $\mathrm{Im}\, T_+(E')$ to duplicate the correct slope at each branch point as given in Sec. 2.2. However, the presence of spurious spikes is a minor detail because they would be removed anyway on going slightly off the real-energy axis.

In spite of the drawbacks mentioned above, it should be plain that the main features of diffraction amplitudes can be reproduced by a simple expression like Eq. (22) or some variant of it. The significance of this result may be appreciated in the light of the discussion of the two-beam case in Section I. It means that for bare-substrate models it is possible to determine the diffraction amplitude function from empirical information only — diffraction intensities[1] and data pertaining to inelastic scattering — and without appeal to detailed model calculations. The power of such a procedure would be enhanced if the substrate band structure were known well enough to identify the inactive segments (Section 2.3).

Acknowledgments

Thanks are due to J. I. Gersten for helpful discussions and to J. A. Appelbaum for reading the manuscript and making a number of constructive suggestions.

[1] J. I. Gersten and E. G. McRae, Surface Science, submitted Sept. 1971.

[2] The bare-substrate model has been found to give results in good agreement with observed intensity-energy curves in cases in which the necessary computations have been carried out. See for example: G. Capart, Surface Sci. **26**, 429 [1971]; D.W. Jepsen, P. M. Marcus and F. Jona, Phys. Rev. Letters **26**, 1365 [1971]; S. Y. Tong and T. N. Rhodin, Phys. Rev. Letters **26**, 711 [1971]; J. B. Pendry, to be published (the bare-substrate model is called "ion-core" model by Pendry). The use of an image potential rather than a step function to represent the surface causes changes in the details of computed intensity curves (mainly details associated with resonances) but does not affect the main features: P. J. Jennings, Surface Sci. **25**, 513 [1971].

[3] The relevant formula reads

$$T = s + (-1)^m (s^2 - 1)^{1/2}$$

where

$$s \equiv -\sin(K_0 d + \varphi)/|\varrho|\,,$$

K_0 being the projection of the primary-wave propagation vector on the inward surface normal, d the atom-layer spacing, φ the phase of the amplitude transmission coefficient of a single atom layer and ϱ the amplitude reflection coefficient of an atom layer. The integer m determined by

$$m\pi \leqq K_0 d + \varphi + \arcsin|\varrho| \leqq (m+1)\pi\,.$$

Formulas like the above appear in many places; see e.g. E. G. McRae, Surface Sci. **25**, 491 [1971], Appendix.

[4] C. M. K. Watts, J. Phys. C **1**, 1237 [1968]. The identity referred to appears on p. 1241 of Watt's paper.

[5] P. J. Jennings and E. G. McRae, Surface Sci. **23**, 363 [1970].

[6] I. S. Gradshteyn and I. M. Ryzhik, Table of Integrals Series and Products, 4th Ed., Academic Press, New York, 1965. Integral number 3.644.4.

[7] J. C. Slater, Phys. Rev. **51**, 840 [1937].

The Optical Potential in Electron Diffraction

A. Howie and R. M. Stern *

Cavendish Laboratory, Cambridge, England

(Z. Naturforsch. **27 a**, 382—389 [1972]; received 4 December 1971)

Dedicated to Prof. Dr. K. Molière *on the occasion of his 60-th birthday*

Expressions are derived for the optical potential and related mean free path as a function of energy in the range 20 eV to 100 keV for electrons and estimates are made of the contributions from the electronic excitations, thermal diffuse scattering and disorder scattering in Al, Cu and Au.

Introduction

The significance of the limited penetration of Bloch waves in real crystals was appreciated and the consequences for the angular position and width of the reflected intensity considered comparatively early in the development of electron diffraction theory [1-3]. The concept of a complex potential ($V = \sum_g V_g^{\,r} + i V_g^{\,i}$), already used in the quantum theory of scattering by Dirac [4], was introduced by Slater [5] and independently by Molière [6] as a convenient phenomenological device for handling such absorption effects in electron diffraction. At this stage, when the theoretical and experimental emphasis was on reflection diffraction at high energies, attention was focussed on the background absorption effect associated with a mean free path (Λ = intensity attenuation distance) related to $V_0^{\,i}$, the average value of the imaginary part of the optical potential: $\Lambda = \hbar v/2 V_0^{\,i}$, where v is the electron velocity **.

Some fifteen years later the development of transmission electron diffraction and electron microscopy techniques allowed more direct observations of the effect of absorption on the fine structure of diffraction spots [7], the attenuation of Pendellösung fringes [8, 9], and the form of extinction contours [9] and convergent beam patterns [10]. In addition to the background absorption effects associated with $V_0^{\,i}$. anomalous absorption effects associated with the Fourier components $V_g^{\,i}$ of the imaginary part of the optical potential became apparent. The variation in the attenuation of different Bloch waves is determined by the form of the periodic intensity distribution of the particular Bloch wave field: the proper development of any theory of electron diffraction therefore requires knowledge of the details of the appropriate optical potential.

The basic theory of the complex potential was given by Yoshioka [11], who using the Thomas-Fermi model, specifically considered the contributions to the real and imaginary part of the optical potential by electronic excitations. In his notation

$$C_{00}^{\,r} = V_0^{\,r}\,,\quad C_{00}^{\,i} = V_0^{\,i}\,,\quad C_{0g}^{\,r} = V_g^{\,r}\,,\quad C_{0g}^{\,i} = V_g^{\,i}\,.$$

Yoshioka's theory was further developed for electronic excitations [12] and for thermal diffuse scattering [13, 14] by a number of authors. In addition, Hall

Reprint requests to Dr. A. Howie, Cavendish Laboratory, Department of Physics, University of Cambridge, *Cambridge*, England.

* On leave from Department of Physics, Polytechnic Institute of Brooklyn.

** At nonrelativistic energies, $\Lambda = 2\,E^{1/2}/V_0^{\,i}$ with E and $V_0^{\,i}$ in eV, Λ in Å.